Partially Unfolded States of β_2-Microglobulin and Amyloid Formation in Vitro[†]

Victoria J. McParland,[‡,§] Neil M. Kad,[‡,§] Arnout P. Kalverda,[‡] Anthony Brown,[#] Patricia Kirwin-Jones,[#] Michael G. Hunter,[#] Margaret Sunde,[⊥] and Sheena E. Radford*[,‡]

School of Biochemistry and Molecular Biology, University of Leeds, Leeds LS2 9JT, U.K., British Biotech Pharmaceuticals Ltd., Watlington Road, Oxford OX4 5LY, U.K., and Department of Biochemistry, University of Cambridge, Tennis Court Road, Cambridge CB2 1GA, U.K.

Received February 4, 2000; Revised Manuscript Received May 2, 2000

ABSTRACT: Dialysis-related amyloidosis (DRA) involves the aggregation of β_2-microglobulin (β_2m) into amyloid fibrils. Using Congo red and thioflavin-T binding, electron microscopy, and X-ray fiber diffraction, we have determined conditions under which recombinant monomeric β_2m spontaneously associates to form fibrils in vitro. Fibrillogenesis is critically dependent on the pH and the ionic strength of the solution, with low pH and high ionic strength favoring fibril formation. The morphology of the fibrils formed varies with the growth conditions. At pH 4 in 0.4 M NaCl the fibrils are ∼10 nm wide, relatively short (50−200 nm), and curvilinear. By contrast, at pH 1.6 the fibrils formed have the same width and morphology as those formed at pH 4 but extend to more than 600 nm in length. The dependence of fibril growth on ionic strength has allowed the conformational properties of monomeric β_2m to be determined under conditions where fibril growth is impaired. Circular dichroism studies show that titration of one or more residues with a pK_a of 4.7 destabilizes native β_2m and generates a partially unfolded species. On average, these molecules retain significant secondary structure and have residual, non-native tertiary structure. They also bind the hydrophobic dye 1-anilinonaphthalene-8-sulfonic acid (ANS), show line broadening in one-dimensional ^{1}H NMR spectra, and are weakly protected from hydrogen exchange. Further acidification destabilizes this species, generating a second, more highly denatured state that is less fibrillogenic. These data are consistent with a model for β_2m fibrillogenesis in vitro involving the association of partially unfolded molecules into ordered fibrillar assemblies.

A number of proteins have been shown to aggregate into amyloid fibrils in vivo, leading to a pathological disorder known as amyloidosis (*1*). This term is generically applied to diseases that involve the conversion of normally soluble proteins or peptides into insoluble fibrillar arrays, although the clinical manifestations of each disease are specific to the identity of the aggregating protein. One such disorder, known as dialysis-related amyloidosis (DRA), involves the aggregation of full-length, wild-type, human β_2-microglobulin (β_2m) into amyloid fibrils (*2*, *3*). As its name implies, DRA arises in patients with chronic renal failure and results in the deposition of β_2m amyloid fibrils systemically (*4*), most typically in the musculo-skeletal system. The disease is a common and serious complication of long-term hemodialysis, with deposits of β_2m amyloid developing in joints within 18 months of the commencement of dialysis (*5*). Serious complications develop in more than 90% of patients undergoing dialysis for a period of 10 or more years (*6*). Clinical symptoms of the disease include carpal tunnel syndrome, destructive arthropathy, and pathological bone fractures.

β_2m is the light chain of the type I major histocompatibility complex. The protein is small (99 residues in length) and nonpolymorphic, and its 7-stranded β-sandwich structure is typical of proteins in the immunoglobulin superfamily (Figure 1). The two β-sheets are linked by a single disulfide bond (*7*). In vivo, β_2m is continuously shed from the surface of cells displaying MHC class I molecules. It is then carried in the plasma to the kidneys, where it is degraded and excreted. As a consequence of renal failure, the β_2m levels accumulate in the plasma [its concentration increases 25−35-fold (*8*)]. Together with a possible multitude of other factors, including the age of the patient and the duration of dialysis, pathogenic amyloid fibrils are formed (*6*, *9*). Analyses of β_2m fibrils extracted ex vivo have identified full-length, as well as truncated, versions of the wild-type protein (*2*−*4*, *10*), β_2m modified with advanced-glycation end products, glycosaminoglycans (*11*), and auxiliary proteins such as apoE and serum amyloid P component (*12*−*14*). In addition, amyloid deposits have been observed in patients prior to the initiation of dialysis, suggesting that the process

[†] We acknowledge with thanks financial support from The University of Leeds, The Wellcome Trust, and the BBSRC. V.J.M. and N.M.K. are supported by the BBSRC, A.P.K. is funded by The Wellcome Trust, and M.S. is a Royal Society University Research Fellow. V.J.M., N.M.K., A.P.K., and S.E.R. are members of the Astbury Centre for Structural Molecular Biology, which is part of the North of England Structural Biology Centre and is funded by the BBSRC.

* To whom correspondence should be addressed. Phone: +44 113 233 3170. Fax: +44 113 233 3167. E-mail: s.e.radford@leeds.ac.uk.

[‡] University of Leeds.

[#] British Biotech Pharmaceuticals Ltd.

[⊥] University of Cambridge.

[§] These authors contributed equally to this work.

[1] Abbreviations: β_2m, human β_2-microglobulin; SAP, serum amyloid component-P; thio-T, thioflavin-T; ANS, 1-anilinonaphthalene-8-sulfonic acid; DRA, dialysis-related amyloidosis; EM, electron microscopy; TTR, transthyretin.

10.1021/bi000276j CCC: $19.00
Published on Web 07/01/2000

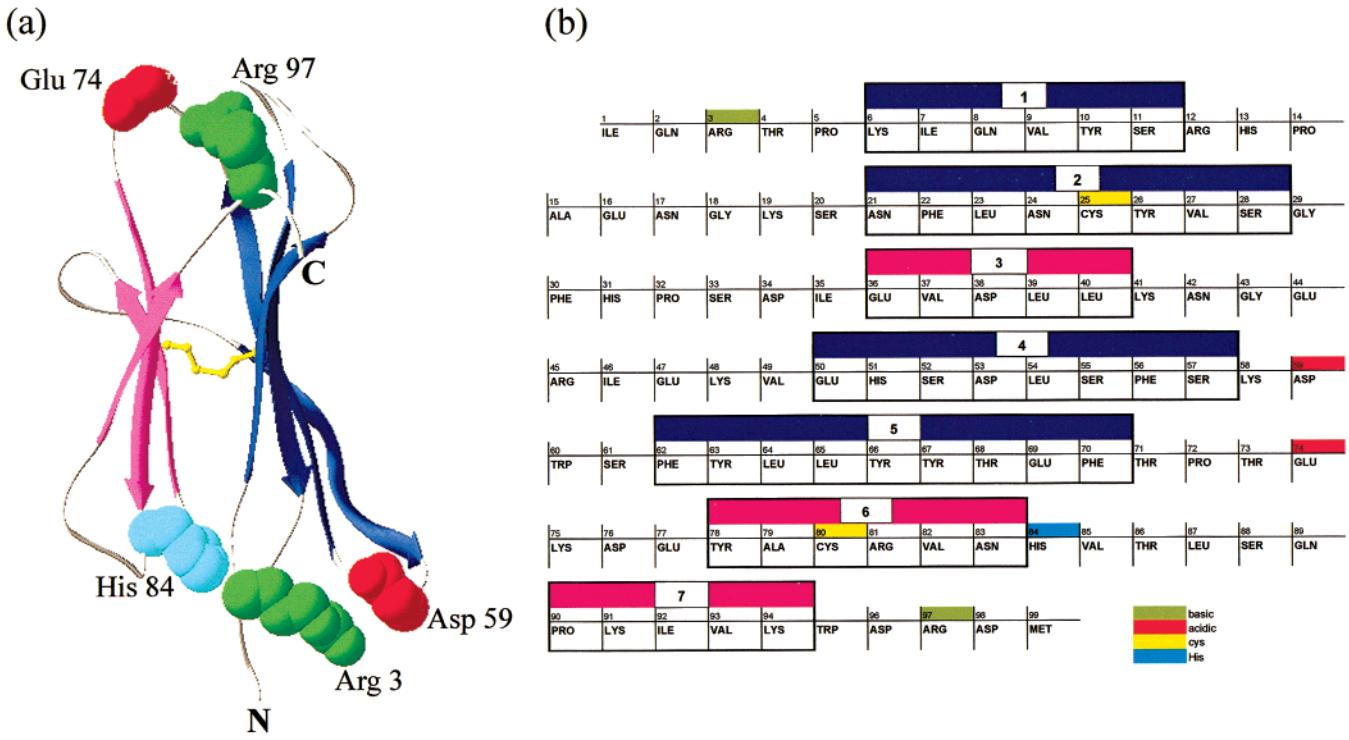

FIGURE 1: Primary and tertiary structural features of β_2m. (a) Ribbon diagram of the X-ray crystal structure of human β_2m (*7*). The positions of the β-strands are taken from NMR measurements of the isolated monomeric protein in solution (*45*). The two β-sheets of this β-sandwich protein are colored blue and purple. The intersheet disulfide bond connecting residues 25 and 80 is shown in yellow. Residues involved in salt bridges in native β_2m that we speculate may be involved in the acid denaturation of the native protein are shown as space-filling representations. Acidic residues are shaded red, arginine residues are colored green, and His84 is shown in blue. (b) The amino acid sequence of human β_2m. The seven β-strands which make up the β-sandwich fold and the residues hypothesized to be important in pH-induced conformational changes shown in panel (a) are highlighted.

of dialysis itself is not a primary factor in the disease (*15*).

Although the sequence and structure of proteins that are involved in amyloid diseases are unrelated, amyloid fibrils share a common structure involving the ordering of β-strands perpendicular to the fiber long axis into an array commonly known as a cross-β structure (*16*). Fibrils are typically ~10 nm in diameter, long, and unbranching and are formed from simpler units known as protofilaments and filaments that intertwine to form the rope-like structure typical of amyloid fibrils (*17*−*20*). As well as having a distinct X-ray fiber diffraction pattern, amyloid fibrils are identified by their unique ability to bind the dye Congo red, producing a characteristic shift in its absorbance spectrum and a green birefringence when viewed through cross-polarizers (*21*, *22*). In addition, fibrils also bind the dye thioflavin T (thio-T), resulting in a characteristic fluorescence emission at 480 nm (*23*, *24*).

Understanding the mechanism of fibrillogenesis is fundamentally important, not only for insight into protein structure and dynamics but also for developing inhibition strategies against amyloid diseases. Delineating how normally soluble, native proteins transform into the ordered array of β-strands typical of amyloid is a crucial first step toward this goal. For intact proteins that form amyloid, current views suggest that unfolding the native protein to form partially unfolded species or more highly denatured states could be a key step in the early stages of the polymerization process. Studies of lysozyme (*25*), transthyretin (TTR) (*26*, *27*), immunoglobulin light chains (*28*−*30*), prions (*31*−*33*), and proteins not involved in amyloid disease (*34*, *35*) have shown that conditions or mutations that destabilize the native protein relative to partially unfolded forms favor fibrillogenesis in vitro. By contrast, for gelsolin, fibrillogenesis has been proposed to involve the self-assembly of more highly denatured conformers (*36*).

Since the first identification of β_2m in DRA 15 years ago (*4*), a wealth of information has been amassed regarding the formation of β_2m fibrils in vivo (*2*, *10*, *12*−*14*). Alongside this, studies of β_2m fibrillogenesis in vitro have shown that amyloid fibrils can be generated from monomeric β_2m purified from human sources (*11*, *37*, *38*). These involved the dilution of β_2m from phosphate-buffered saline (pH 7.4) into distilled water, followed by its reconcentration (*37*). In an extension of these studies, Ono and Uchino (1994) suggested that SAP may play a crucial role in the formation of the amyloid-like fibrils of β_2m. Finally, Naiki et al. (1997) demonstrated that ex vivo fibrils of β_2m can be elongated using monomeric protein under acidic conditions. Despite these studies, relatively little is known about the mechanism of β_2m amyloidosis at a molecular level. Here we present a systematic study of the conditions favoring β_2m fibrillogenesis in vitro and relate these findings to the conformational properties of the monomeric precursor protein. We show that fibrils of β_2m can be formed in vitro by incubation of recombinant, full-length, wild-type protein at low pH and high ionic strength. Under these conditions, partial unfolding of the β_2m is favored. The data show that β_2m conforms with models for amyloid formation based on studies of other proteins (*25*, *26*, *28*−*30*, *32*−*35*) in that partial unfolding of the native protein precedes amyloidosis.

MATERIALS AND METHODS

Materials. Ampicillin, Q-Sepharose, and all other AnalaR reagents were purchased from Sigma Chemical Co. Butyl-Sepharose and Superdex 75 were purchased from Pharmacia. Carbenicillin was purchased from Melford Chemicals.

β_2m Overexpression and Purification. Two different expression systems were used to produce human β_2m. Material isolated using each system behaved identically in all of the experiments carried out. In the first system, β_2m was overexpressed as a soluble protein in *Pichia pastoris* by placing cDNA encoding full-length human β_2m under the control of the methanol-inducible alcohol oxidase promoter. Following induction with methanol, the β_2m was secreted into a basal salt medium in fermenters at a concentration of 1 g/L. The secreted protein was purified by hydrophobic interaction chromatography on a butyl-Sepharose column equilibrated with 10 mM sodium phosphate buffer and 2 M $(NH_4)_2SO_4$, pH 7.0. The column was washed with 10 column volumes of equilibration buffer, and protein was then eluted with 10 mM sodium phosphate buffer and 50% (v/v) ethylene glycol, pH 7.0. β_2m-containing fractions were pooled and further purified on a Superdex 75 column equilibrated with 0.5 M NH_4HCO_3.

β_2m was also produced by overexpression in *E. coli* using the plasmid pHN1+ (*39, 40*). TG1-competent cells were transformed by the plasmid and grown on Luria broth in the presence of carbenicillin (250 μg/mL). Cultures were grown at 37 °C for 18 h without induction of protein expression and were harvested by centrifugation. Overexpressed β_2m was sequestered in the cells as inclusion bodies. These were isolated using standard procedures (*41*). The inclusion bodies were washed five times with 10 mM Tris-HCl, pH 8.0, and resuspended in 10 mM Tris-HCl, pH 8.0, containing 8 M urea for 1 h at 4 °C. Insoluble material was removed by centrifugation, and the solubilized β_2m was then refolded by dialysis into 10 mM Tris-HCl, pH 7.0, at 4 °C. β_2m was then purified essentially as previously reported (*42*). Material produced in *P. pastoris* and *E. coli* was stored as a lyophilized powder. The protein was shown to be authentic β_2m by mass spectrometry; the two systems produced protein that differs only in the presence of an additional methionine at the N-terminus of the material produced in bacteria.

Thioflavin-T Binding Studies. A final β_2m concentration between 0.5 and 1.0 mg/mL was used in all measurements. A composite buffer was used throughout. In experiments over the range pH 5.0−1.6, a buffer consisting of 50 mM sodium acetate and 50 mM glycine was used. For experiments performed at higher pH values, the glycine was replaced with 50 mM sodium phosphate. In all cases, NaCl was added to each buffer mixture to adjust the ionic strength to a fixed value of 400 mM at each pH. In these experiments, a stock solution of native β_2m was prepared from the lyophilized protein. This solution was then passed through a 0.2-μm filter and diluted to the desired final conditions. The protein was incubated at 37 °C for 72 h without stirring, after which time 10-μL aliquots were removed, added to a thio-T solution (10 μM final concentration) at pH 8.5, and buffered using 50 mM Tris-HCl. Thio-T binding was measured by averaging the emission signal over 20 s using a PTI Quantamaster C-61 spectrofluorimeter set at 444 nm (excitation) and 480 nm (emission). Control experiments showed that the fibrils formed at lower pH values were stable at pH 8.5 over the time-course of the measurements. The fluorescence of the thio-T alone was also measured at each pH, and the value was subtracted from that value found in the presence of protein. In experiments to measure the initial rate of fibrillogenesis, β_2m (0.59 mg/mL) was prepared as described above, thio-T (final concentration, 10 mM) was added, and fibrillogenesis was measured continuously by fluorescence at 480 nm. Control experiments in which aliquots of the reaction mixture were removed and added to a thio-T-containing assay buffer at different times after the initiation of fibril growth showed that the dye had no effect on the growth rates. No lag phase was observed at the protein concentrations used. The initial rate of fibril growth was reproducible over several replicates.

Electron Microscopy. Colloidon-coated copper EM grids were placed coated-side-down for 30 s onto sample drops containing the preformed β_2m fibrils. The grids were then retrieved, excess solvent was removed by blotting with filter paper, and the sample was stained with 4% (w/v) uranyl acetate for 30 s. Grids were then blotted again and air-dried before analysis. All images were taken using a Philips CM10 electron microscope operating at 100 keV.

Fiber Diffraction. β_2m fibrils were grown for 2 weeks by incubation of 5 mg/mL protein at pH 1.6 and 37 °C at an ionic strength of 400 mM. Under these conditions, the fibrils form a viscous gel. The samples were centrifuged at 13 000*g* for 10 min, resulting in the sedimentation of a noticeably more viscous layer to the base of the Eppendorf tube. This layer was mixed with an equal volume of 20 mM HCl and centrifuged at 10 000*g* for another 10 min. The viscous layer sedimented by this procedure was used for further preparation of samples for diffraction studies. Fibrils grown in 20 mM sodium acetate buffer at pH 3.6 in the absence of NaCl were centrifuged at 13 000*g* for 10 min and then were resuspended in a minimum of growth solution. Droplets of the two different fibril-containing solutions were suspended between the ends of two wax-filled glass capillaries and were allowed to air-dry, yielding clumps of partially aligned fibrils. X-ray fiber diffraction patterns were collected at the Department of Biochemistry, University of Cambridge, using a Rigaku Cu Kα rotating-anode source (wavelength, 1.5418 Å) and an R-AXIS IV image-plate X-ray detector.

Congo Red Birefringence. Drops of fibril-containing solutions were air-dried on gelatin-coated slides. Fibrils produced in vitro by a 10-residue peptide with the sequence of the A-strand of TTR and known to form amyloid fibrils (*43*) were used as a positive control. The procedure for Congo red staining of the samples was adapted from that given in ref *22*. The slides were incubated for 15 min in 80% (v/v) ethanol containing 4% (w/v) NaCl and 0.01% (w/v) NaOH and then were allowed to air-dry. This was followed by incubation for 15 min in 80% (v/v) ethanol containing 2% (w/v) Congo red, 4% (w/v) NaCl, and 0.01% (w/v) NaOH. The slides were then washed in 100% ethanol 3 times and were allowed to dry before being examined between cross-polarizers on a Leica MZ6 stereo-zoom microscope.

Circular Dichroism (CD). CD experiments were performed on a Jasco J715 CD spectropolarimeter. For measurements in the far-UV (190−260 nm), the CD signal was recorded in a 1-mm path-length cell using a protein

concentration of 0.4 mg/mL. For measurement in the near-UV region (250−350 nm), CD spectra were recorded using the same protein concentration and a 1-cm path-length cuvette. pH titration of β_2m was carried out by monitoring the CD signal of the protein at 220 nm as a function of pH. For this and other experiments involving titration with acid using optical methods, a composite buffer containing 25 mM sodium phosphate and 25 mM sodium acetate was used. Together, these provide buffering capacity over a wide pH range [phosphate has two pK_a's of relevance (2.15, 7.20) and acetate has one (4.76)]. After acidification, protein samples were incubated at the required temperature for 30 min and the CD signal was then measured. Measurements at 220 nm were recorded for 1 min with a 1-nm bandwidth and interval and response times of 1 and 8 s. The data for each pH were subsequently averaged.

Assuming that the transitions are fully reversible and that one or more residues with a similar pK_a are involved in each of two transitions,

$$X + mH^+ \leftrightarrow XH_m^+ + nH^+ \leftrightarrow XH_{n+m}^+$$

the data were fitted to:

$$CD^{220} = \frac{I_1[H^+]^{m+n} + I_2K_1[H^+]^m + I_3K_1K_2}{[H^+]^{m+n} + K_1[H^+]^m + K_1K_2} \quad (1)$$

where I_1, I_2, and I_3 are the CD signals of acid-denatured, partially unfolded, and native β_2m, respectively; K_1 is the equilibrium constant between X and XH^+_n; and K_2 is the equilibrium constant between XH^+_n and XH^+_{n+m}. $[H^+]$ is the concentration of hydrogen ions, m is the number of hydrogen ions bound in the first transition, and n is the number of hydrogen ions bound in the second transition. In the fit to the experimental data in Figure 9a, m and n were free-floated and were determined to be 1.45 and 0.67, respectively. A similar analysis to this has been used previously (*44*).

ANS Binding. The fluorescence emission spectra of 1-anilinonaphthalene-8-sulfonic acid (ANS) with and without the protein were recorded on a Photon Technology International Quantamaster C-61 spectrofluorimeter at 15 °C. Protein samples (0.01 mg/mL) in composite buffer were diluted 10-fold into the same buffer containing ANS (final concentration, 250 μM) at the appropriate pH value. The ANS fluorescence was then read immediately using an excitation wavelength of 389 nm, and the fluorescence emission was collected between 400 and 600 nm using slit widths of 5 nm. The fluorescence emission of ANS in buffer alone was then subtracted from that obtained in the presence of β_2m. The experiment was repeated at 25 and 37 °C. In each case, the data were qualitatively similar to those obtained at the lower temperature. Control experiments using thio-T showed that fibrils did not form during the time-course of this experiment. The results obtained were independent of the protein concentration (0.01−0.24 mg/mL β_2m) and the precise composition of buffer salts used (experiments using protein dissolved in the absence of buffer salts, in 20 mM sodium acetate, in 20 mM sodium phosphate buffer, or in the composite buffer were identical).

NMR Spectroscopy. ^{1}H NMR spectra were recorded at 15 °C on a Varian Inova 500-MHz NMR spectrometer. The samples contained 4 mg/mL β_2m dissolved in D_2O. The sample did not contain additional buffer salts (to inhibit protein polymerization) and was brought to the desired pH by the addition of small amounts of DCl or NaOD. ^{1}H NMR spectra were acquired using a 40-Hz presaturation field during the 1.5-s recycle delay to suppress the residual water signal. The spectral width was 7500 Hz, and 1024 scans were averaged. For hydrogen-exchange experiments, lyophilized β_2m was dissolved in D_2O at the appropriate pH, and one-dimensional ^{1}H NMR spectra were acquired at 15 °C using a spectral width of 8000 Hz and a recycle delay of 1.5 s; 1024 scans were averaged for spectra acquired at pH 7.0, and 256 scans were taken for spectra obtained at pH 4.0. The first spectrum was taken 10 min after the addition of D_2O, and each spectrum took either 35 (at pH 7.0) or 9 min (at pH 4.0) to acquire. All data were processed using FELIX 2.3 (Biosym Technologies, San Diego). The number of protected sites remaining at each time was determined by integration of the amide and aromatic regions of the one-dimensional ^{1}H NMR spectrum, followed by normalization to the intensity of the upfield-shifted methyl resonances between −0.4 and −0.6 ppm [which contains the Leu23 $C^{\delta}H_3$ and Ile35 $C^{\delta 1}H_3$ resonances (*45*)]. The contribution from the nonexchanging hydrogens that resonate downfield of the water signal was then subtracted. The rate of hydrogen exchange predicted for an unstructured polypeptide of the sequence of human β_2m at pH 4.0 and 15 °C was calculated using the parameters determined in ref *46*.

RESULTS

β_2m Fibrillogenesis in Vitro. The amyloidogenicity of purified β_2m (0.95 mg/mL) was first evaluated as a function of pH over the range 7.0−1.6 (total ionic strength of 400 mM). The samples were incubated for 72 h at 37 °C at the required pH, without stirring, as described in the Materials and Methods section, and the presence of fibrils was detected by a number of methods including thio-T fluorescence, Congo red binding, turbidity (at 350 nm), and EM. The results, using thio-T as a specific probe for amyloid formation, are shown in Figure 2a. Interestingly, at pH 5.0 and above, no fibrils were detected by any method. Below pH 5.0, however, amyloid fibrils were formed over a wide pH range. The extent of fibrillogenesis was similar over the range pH $\sim$ 4.0−1.5. Kinetic experiments showed that, although the rate of fibril formation is dependent on the pH (see below and Table 1), the fibrillogenesis was essentially complete within 72 h under the conditions employed. The fibrils formed bind Congo red, producing the characteristic red-shifted absorbance spectrum of the dye typically observed during amyloid formation (*21*). Attempts were also made to detect the characteristic green birefringence of Congo red bound to the fibrils of β_2m which are formed at pH 1.6 and 4.0. Fibrils grown at pH 1.6 at an ionic strength of 0.4 M showed the green birefringence characteristic of ordered amyloid fibrils. The fibrils grown at higher pH values, however, did not appear to give birefringence. This may have been due to difficulties in concentrating these fibrils by centrifugation, and consequently, the concentration of these fibrils may have been too low to yield sufficient oriented-dye molecules to impart birefringence.

As well as being highly dependent on the pH of the solution, β_2m fibrillogenesis is also highly dependent on the

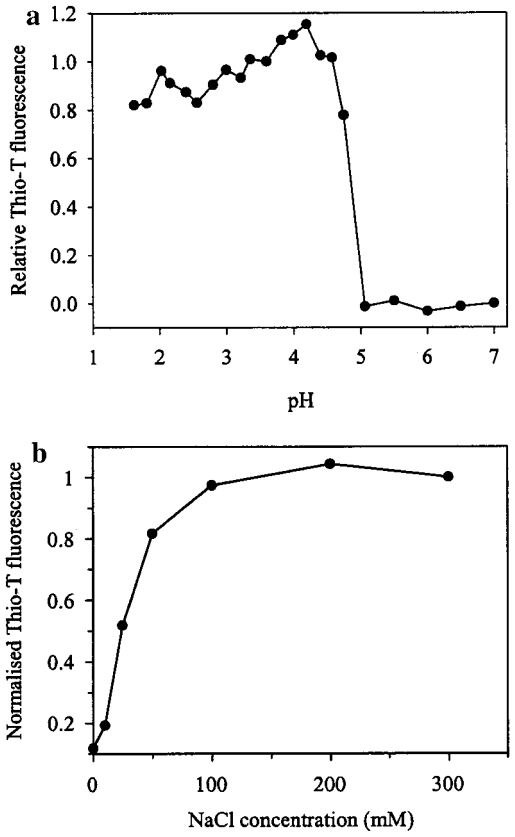

FIGURE 2: Fiber growth of β_2m measured by thio-T fluorescence. (a) The pH dependence of β_2m fibrillogenesis. β_2m (0.59 mg/ml) was incubated at the pH values shown for 72 h at 37 °C, after which time its ability to bind thio-T was measured. The data were scaled by taking the thio-T fluorescence value at pH 7 as zero and the value at pH 3.6 as unity and scaling all other values accordingly. (b) The ionic strength dependence of β_2m fibrillogenesis. β_2m (0.59 mg/mL) was incubated at pH 3.4, 37 °C, at the ionic strengths indicated for 72 h, after which time the samples were assayed for extent of fibrillization using thio-T as described in the Materials and Methods section. The fluorescence of thio-T was normalized by subtracting the buffer and scaling the data relative to the value obtained at 300 mM.

ionic strength (Table 1 and Figure 2b). At an ionic strength of 8 mM (equivalent to the ionic strength of the composite buffer without additional NaCl), no fibrils are observed under the conditions used. By contrast, at the same pH at an ionic strength of >50 mM, the fibril growth is rapid (Table 1) and complete, reaching a plateau value identical to that formed at higher ionic strengths after an incubation time of 72 h. In addition to its sensitivity to the pH and ionic strength, β_2m fibrillogenesis is also highly dependent on the protein concentration. The rates increase with increasing concentration (Table 1), as expected for a multimolecular association event, and with temperature (Table 1).

The Morphology of β_2m Fibrils Varies with pH. The data in Figure 2a show that fibrils of β_2m form below pH 5 under a range of solution conditions. To examine the morphology of the fibrils formed at different pHs, negative-stain EM images of the fibrils grown from solutions of β_2m incubated in 0.4 M NaCl at 37 °C for 3 days over a range of pH values were analyzed. Typical images are shown in Figure 3. In all cases, the fibrils formed are ~6−10 nm in diameter, similar to the width of the fibrils formed from other amyloidogenic proteins (*43*). No fibrils were observed above pH 4.6 (Table 1), in agreement with the results shown in Figure 2a. At pH 3.4, the fibrils formed are relatively short (ranging between 50 and 200 nm in length) and curvilinear. At the more acidic pH values, however, the fibrils are longer; at the lowest pH studied (pH 1.6) fibrils exceeding 600 nm in length were routinely seen. Thio-T binding indicates that approximately the same total amount of fibrillar material is formed at each pH below 5.0 (Figure 2a). This suggests that at pH 3.4 many short fibrils form, whereas at pH 1.6, fewer, much longer fibrils develop.

Table 1: Effect of Growth Conditions on the Morphology and Initial Rate of β_2m Fibril Formation

condition[a]		rate of fibril formation[b]	fibril length (nm)	thio-T binding	fibril morphology
pH	1.6	28.4	200−1000	yes	curved
	3.4	83	≥100	yes	curved
	4.6	0	none	yes	aggregate[c]
concn	0.09	13.4	≥100	yes	curved
	0.18	24.1	≥100	yes	curved
	1.41	195.5	≥100	yes	curved
salt	50	20.8	≥100	yes	curved
	100	33.4	≥100	yes	curved
	400	83	≥100	yes	curved
temp[d]	20	1.7	≥100	yes	curved
	26.5	3.4	≥100	yes	curved
	30.4	3.8	≥100	yes	curved

[a] Concn refers to the mg/mL concentration of β_2m (when not specified, β_2m concentration used was 0.59 mg/mL), and salt concentration is expressed in mM final ionic strength (when not specified, the ionic strength was fixed as 400 mM). Temperature is in °C (when not specified, the temperature was fixed at 25 °C). [b] This rate is the initial rate of fibrillogenesis measured in arbitrary units s^{-1}. The values are accurate to within 10% of the calculated value. [c] This aggregate appeared to be amorphous. [d] The pH used was 4.0, and the ionic strength was 208 mM.

The β_2m fibrils formed in vitro are not so straight as those formed from peptides (*47, 48*) and other amyloidogenic proteins, which are typically straight polymers of indeterminate length (*49*). Interestingly, however, β_2m fibrils observed directly in the intracellular lysosome-like corpuscles of mesenchymal cells and macrophages, as well as those extracted from amyloid deposits in patients suffering from DRA, are also relatively short in length (<600 nm), 6−12 nm in diameter, and curvilinear (*4, 50*). In accord with this, X-ray fiber diffraction of the β_2m fibrils grown at pH 1.6, using 5 mg/mL β_2m at 37 °C and 400 mM ionic strength for 2 weeks, show the expected dominant reflection at 4.7 Å on the meridian and associated equatorial reflections at 9 and 15 Å, typical of those expected for fibrils with a cross-β structure (Figure 4). The 9 Å reflection may arise from the intersheet separation perpendicular to the fiber axis, while the 15 Å reflection may reflect the superposition of an interference function which arises from the close packing of subfilaments or protofilaments [(*51*) and L. Serpell and M. Sunde, unpublished data]. In addition, a weak reflection at approximately 34 Å is also observed, which could correspond to the protofilament diameter (not shown). Although cross-sectional analysis of the β_2m fibrils has not been carried out, all other amyloid fibrils examined in this way have been shown to consist of three to six subfilaments, which then associate to form the long, unbranched amyloid fibrils observed by EM (*52*). The data thus confirm that fibrils formed from monomeric recombinant β_2m are, indeed, amyloid.

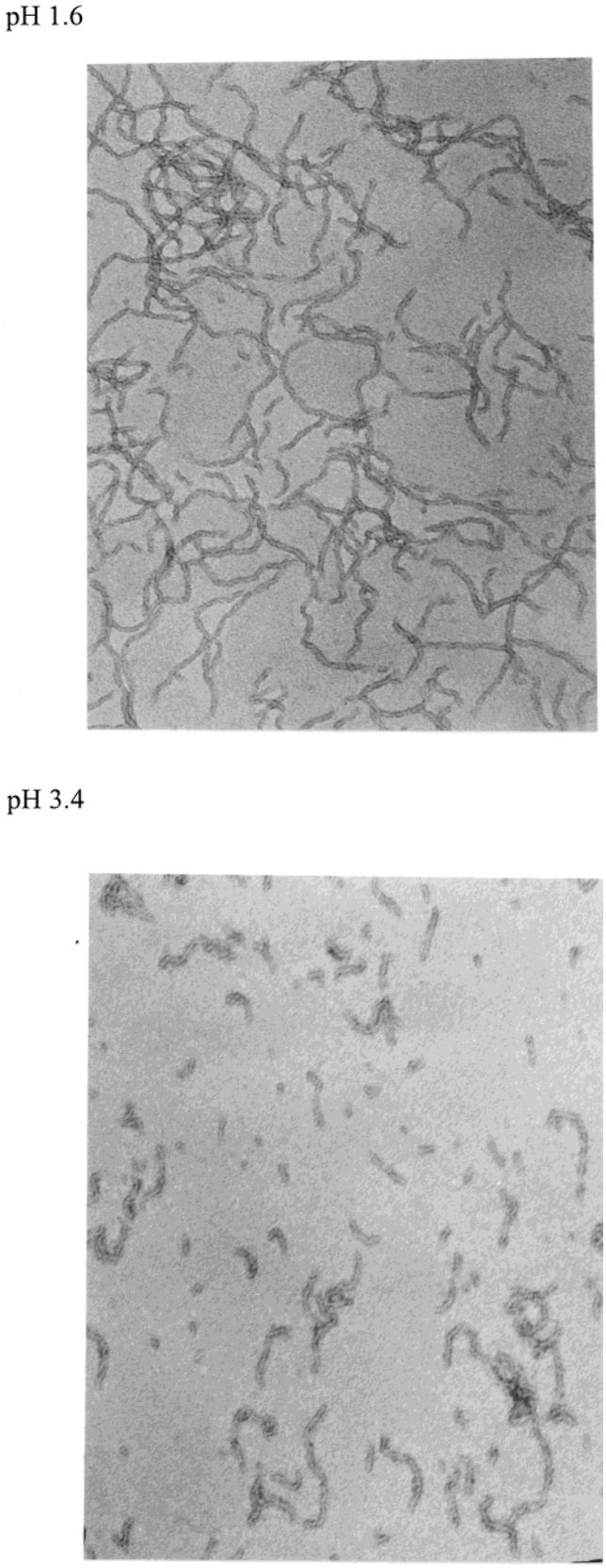

FIGURE 3: Negatively stained EM images of β_2m fibrils formed at pH 3.4 and 1.6. Fibrils were formed by incubating β_2m (0.59 mg/mL) at different pH values at 37 °C as described in the Materials and Methods section. The scale bar represents 100 nm.

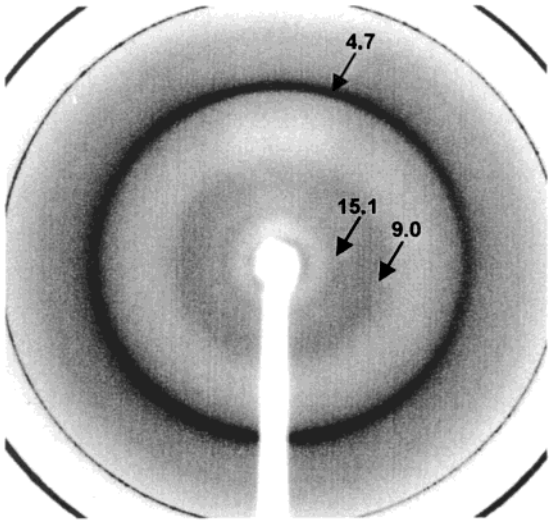

FIGURE 4: X-ray fiber diffraction pattern of β_2m fibrils formed in vitro. The image shows major reflections at 4.7 Å on the meridian and equatorial reflections centered at 9.0 and 15.1 Å. The intense outer rings reflect the presence of residual salt in the sample.

Acid Unfolding of β_2m. The experiments described in Figure 2 have established that β_2m fibrils do not form under conditions of low ionic strength, whereas in the presence of NaCl, fibrils form readily. These observations allow examination of the acid-denaturation process of the β_2m in the absence of protein assembly. The far- and near-UV CD spectra of the β_2m at pH 7.0, 4.0, and 1.2 are shown in Figure 5a,b, respectively. The far-UV CD spectrum of native β_2m obtained at pH 7.0 is very weak in intensity, as often observed for β-sheet proteins (*53*). Nevertheless, clear negative and positive bands are observed at 218 and ~200 nm, respectively, consistent with the known all-β-sheet structure of the native protein (*7*). The near-UV CD spectrum of recombinant β_2m shows positive peaks around 270 and 290 nm, indicating at least some of its aromatic residues are in fixed conformations in the native state. Acidification of the solution to pH 1.2 results in more extensive denaturation of the β_2m, as judged by the large negative peak in the far-UV CD around 200 nm and the lack of a significant signal in the near-UV CD (Figure 5a,b). By contrast, at pH 4.0, the β_2m is only partially denatured. The far-UV CD spectrum of this species has a large negative band centered on 218 nm, suggesting that significant β-sheet secondary structure persists at this pH. The increase in negative intensity at ~218 nm relative to that of the native protein could reflect an attenuation in the contribution of aromatic residues to the far-UV CD spectrum of the protein at these wavelengths. In agreement with this, the tertiary structure of the β_2m is significantly perturbed at this pH, as reflected by a loss of near-UV CD, particularly at 275 nm. The near-UV CD spectrum of the species formed at pH 4.0 cannot be described by the summation of the spectra of the native protein and the acid-denatured state formed at pH 1.2, suggesting that a species with a distinct conformation is populated around pH 4.0.

To investigate further the conformation of the β_2m at low pH, ANS was used to probe the nature of the acid-denaturation transition. This dye binds to regions of exposed hydrophobic surface area in a manner which is characteristic of the formation of partially unfolded species (*54*). Figure 6

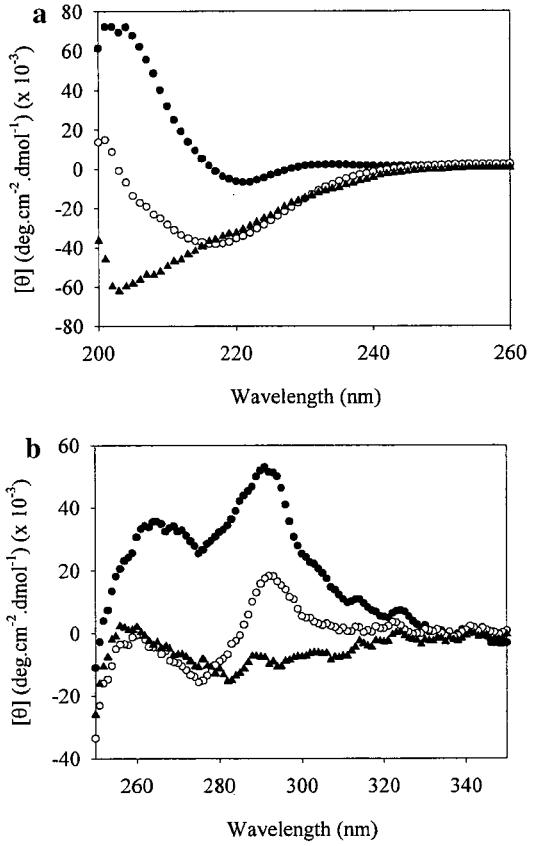

FIGURE 5: Far- and near-UV CD spectra of different conformational states of β_2m: (a) CD spectra of β_2m (0.2 mg/mL) in the far-UV and (b) CD spectra of β_2m (0.4 mg/mL) in the near-UV at 15 °C at pH 7.0 (filled circle), pH 4.0 (open circle), and pH 1.2 (filled triangle).

shows the changes in the ANS fluorescence intensity and its λ_{max} in the presence of β_2m at different pH values. The data show that the ANS does not bind to the β_2m above pH 5.5. By contrast, a pronounced increase in the intensity of the ANS fluorescence, as well as a blue shift in its λ_{max}, are observed at the amyloidogenic pH values between 1.0 and 5.0. These findings, together with the CD data described above, suggest that at least two distinct species are populated during acid denaturation of the β_2m. The first, formed around pH 4.0, retains significant secondary structure and residual non-native packing of aromatic side chains and binds the ANS. The second, formed at lower pH, is more highly denatured. This species retains little or no secondary structure and lacks fixed tertiary interactions, but it is collapsed, at least in that it binds the ANS. Interestingly, fibrils can be formed at both of these pH values at increased ionic strengths (Figure 2a).

NMR Studies of Partially Unfolded β_2m. To investigate the conformational properties of acid-denatured β_2m in more detail, NMR spectra of the protein were acquired at several pH values. Representative one-dimensional ^{1}H NMR spectra are shown in Figure 7. At pH 7.0, the spectrum of β_2m is typical of that of a native protein. The resonances are sharp and well-dispersed (8 upfield methyl resonances are observed between 0.5 and 1.0 ppm). These arise from the side chains of residues Leu23, Val37, Leu40, and Ile35 and are consistent with assignments published previously (*45*). In addition, resonances arising from 37 C^α hydrogens appear between 4.8 and 5.7 ppm, which is indicative of the existence of a

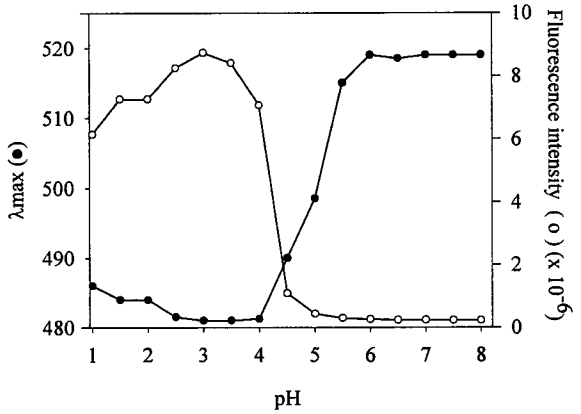

FIGURE 6: ANS binding to acid-denatured β_2m. Monomeric β_2m at the pH values shown was mixed with ANS and the fluorescence emission spectrum of the fluorescent dye monitored (see Materials and Methods). The λ_{max} of the dye and the fluorescence emission intensity at 389 nm are shown.

β-sheet secondary structure (not shown). By contrast, at pH 3.4, the spectrum of β_2m is more typical of that of a partially unfolded state. The chemical shift dispersion is reduced markedly, and the upfield-shifted methyl resonances characteristic of the native state are no longer resolved. In addition, resonances are broadened, presumably reflecting interconversion of molecules in intermediate exchange on the NMR time scale. Sedimentation velocity experiments showed that samples of the β_2m prepared in an identical manner to those used for NMR are more than 95% monomeric, with an M_r of 11 970 (expected M_r = 11 860), ruling out intermolecular association as the reason for the increased line widths observed at acidic pH (V. J. McParland, N. M. Kad, S. E. Radford, A. Baron, G. Howlett, and C. Rieger, unpublished results). In agreement with this, no visible aggregation occurred during data acquisition, nor were fibrils detected by thio-T binding during or after the NMR experiment.

The one-dimensional ^{1}H NMR spectra of β_2m denatured at pH 1.2 and in 7 M urea are also shown in Figure 7. At pH 1.2, the spectrum resembles closely that obtained at pH 3.4. Nevertheless, several resonances have shifts distinct from those of the fully unfolded protein obtained in 7 M urea, and the peaks are broad relative to those in the spectrum of the chemically denatured protein. This suggests that residual structure persists in acid-denatured β_2m, which is consistent with the ability of this species to bind ANS (Figure 6).

To examine whether stable hydrogen bonds persist in different conformational states of β_2m, a series of one-dimensional ^{1}H NMR spectra were obtained at different times after dissolution of the protein in D_2O solution at pH 7.0 and 4.0. At each time point, the integrated area of resonances arising from residual amide hydrogens was measured as described in Materials and Methods. The data (Figure 8) show that native β_2m is highly protected from hydrogen exchange; more than 55 amides remain protected after 3 days in D_2O solution. By contrast, at pH 4.0 exchange is rapid. All amides exchange within ~10 h, even though the intrinsic rate of hydrogen exchange is reduced 1000-fold at pH 4.0 relative to the rate at pH 7.0 (*46*). Interestingly, however, although the majority of amides exchange rapidly in partially unfolded β_2m at pH 4.0 (they exchange within the 10-min dead-time of the experiment), about 30 amides show

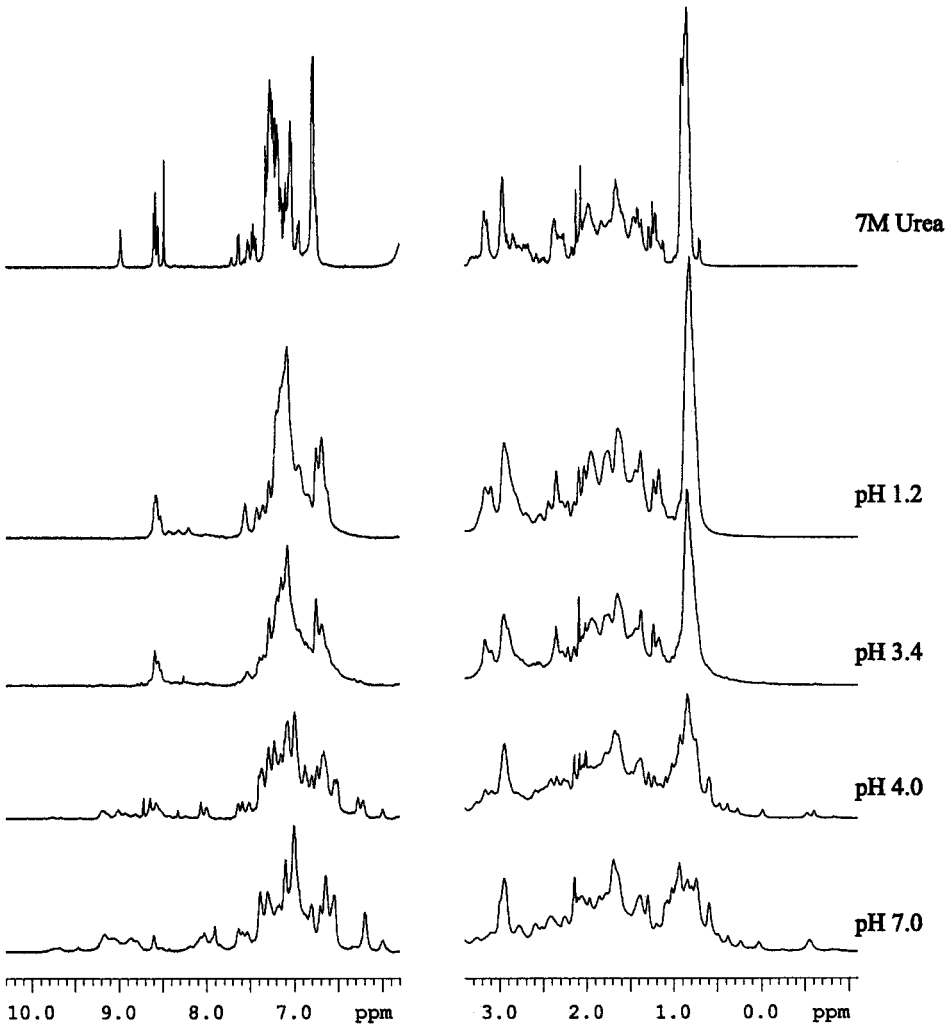

FIGURE 7: Characterization of partially unfolded β_2m by ^{1}H NMR. One-dimensional ^{1}H NMR spectra of β_2m at 15 °C at the pH values shown. β_2m was freshly dissolved in D_2O solution at the required pH values and one-dimensional NMR spectra wereacquired as described in the Materials and Methods section. The spectrum of β_2m denatured in 7 M urea at pH 3.6 is shown for comparison. In this spectrum, the peak at 9.0 ppm arises from an impurity.

significant protection from hydrogen exchange relative to that calculated for an unprotected polypeptide with the sequence of β_2m under these conditions (*46*) (Figure 8).

pH-Mediated Structural Changes and β_2m Amyloidosis. A more detailed investigation of the acid-unfolding transition was carried out by monitoring the CD signal of the β_2m at 220 nm as a function of pH. The data (Figure 9a) show that the β_2m undergoes two transitions over the pH range studied (pH 7.0−1.2). The first involves an increase in the negative ellipticity and describes the equilibrium between native and partially unfolded β_2m. The second transition occurs below pH 3.5 and involves a decrease in negative ellipticity relative to that at pH 3.5. This transition reflects the further unfolding of the partially unfolded molecules and the population of the acid-denatured state. Fitting the data to eq 1 (see Methods and Materials) yields apparent pK_a values associated with the first and second transitions of 4.7 and 3.3, respectively.

To investigate the role of the acid-unfolded states of β_2m in fibrillogenesis, thio-T was added to an aliquot of each sample from the acid titration described above, and fibril formation was measured immediately by monitoring the fluorescence of the dye. These data showed that thio-T does not bind to β_2m at any pH upon its immediate acidification (not shown). Samples were then incubated for 72 h at 25 °C, and aliquots were again assayed for fibril formation by thio-T fluorescence. This time, fibrils were observed between pH 3.0 and 4.5, but not in samples incubated at higher or lower pH values (Figure 9a). The presence of fibrils in the sample incubated at pH 4.0 was confirmed by negative-stain EM and fiber diffraction. The results indicated that fibrils had formed with the cross-β structure typical of an amyloid and the same morphology as those generated at pH 4 in the presence of 0.4 M NaCl (see above). However, these samples did not show green birefringence with Congo red. The extent of fibril formation in the composite buffer (ionic strength, 23 mM) correlates well with the ionic strength dependence of fibrillogenesis shown in Figure 2b. Most importantly, the pH of maximal fibril growth corresponds with the pH at which partially unfolded β_2m is most highly populated, implicating this species as an important amyloid precursor.

Although β_2m is not fibrillogenic below pH 2.5 at low ionic strength, fibrils form readily in this pH range at an ionic strength of 0.4 M (Figure 2a). To investigate this apparent discrepancy, a sample of β_2m was incubated for 3 days at pH 1.5 in the absence of NaCl. After this time, an aliquot was removed and its secondary structure and ability to form fibrils were assessed using far-UV CD and thio-T fluorescence, respectively. As expected, β_2m is unfolded at

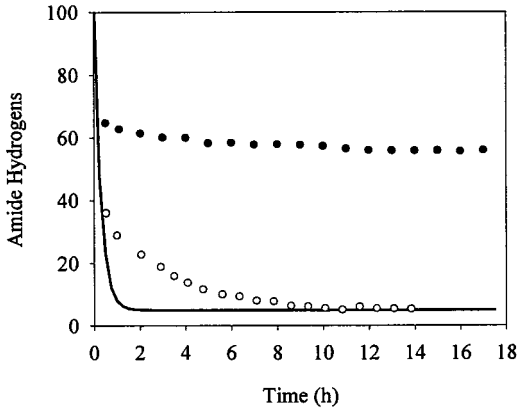

FIGURE 8: Kinetic profiles of hydrogen exchange of β_2m at pH 7.0 and 4.0. β_2m was dissolved in D_2O solution at pH 7.0 (filled circle) and pH 4.0 (open circle), and the rate of hydrogen exchange at 15 °C was determined by collecting a series of one-dimensional ^{1}H NMR spectra at different times after the dissolution, as described in the Materials and Methods section. The solid line depicts the curve predicted for exchange in a sample consisting of 90% of unprotected molecules [calculated using the intrinsic rates of exchange for residues in an unstructured protein with the sequence of β_2m using standard methods (*46*)] and assuming that 10% of molecules are protected from hydrogen exchange in the small population of native molecules that persist under these conditions [assessed by integration of the upfield-shifted methyl resonances that persist at pH 4 (see Figure 6)].

pH 1.5 (Figure 9b) and does not bind thio-T, in agreement with the results shown in Figures 5a and 9a. NaCl (0.4 M) was then added to the initial sample, and its far-UV CD spectrum was again acquired. The results showed that the β_2m had partially refolded under these conditions, forming a species with a CD spectrum similar to that generated at pH 4 in the absence of NaCl (Figure 9b). The sample was then incubated for 1 h further at 25 °C, and thio-T was added. Not surprisingly, the addition of NaCl caused fibrils to form in this sample (Figure 9a), the extent of fibril formation according with that shown in Figure 2a. The results thus suggest that the acid-denatured and partially unfolded forms of β_2m are in equilibrium, but that the latter is fibrillogenic. In agreement with this view, the initial rate of fibrillogenesis is maximal at ~pH 3.6 (Figure 9c).

DISCUSSION

In this paper we have shown that native, monomeric β_2m partially unfolds at acidic pH, forming a species that readily assembles into amyloid fibrils in vitro. The fibrils formed resemble those formed previously in vitro at physiological pH using dialysis methods (*3, 37*) including those formed in the presence of SAP (*11*). Akin to studies on other proteins (*55*−*57*), we show that the morphology of the β_2m fibrils varies with the pH at which they are formed. At pH 1.6, fibril growth is slow, favoring the formation of fewer, longer fibrils. The β_2m fibrils formed in the present study adhere to the classical view of an amyloid. They exhibit a cross-β fiber diffraction pattern, are about 10 nm wide and unbranching (as viewed by EM), bind Congo red and thio-T, and display the classic green birefringence of Congo red characteristic of an amyloid. Nevertheless, they are unusual in that they are curvilinear and are shorter than fibrils formed from other proteins. Interestingly, β_2m fibrils have been observed directly within the intracellular lysosome-like

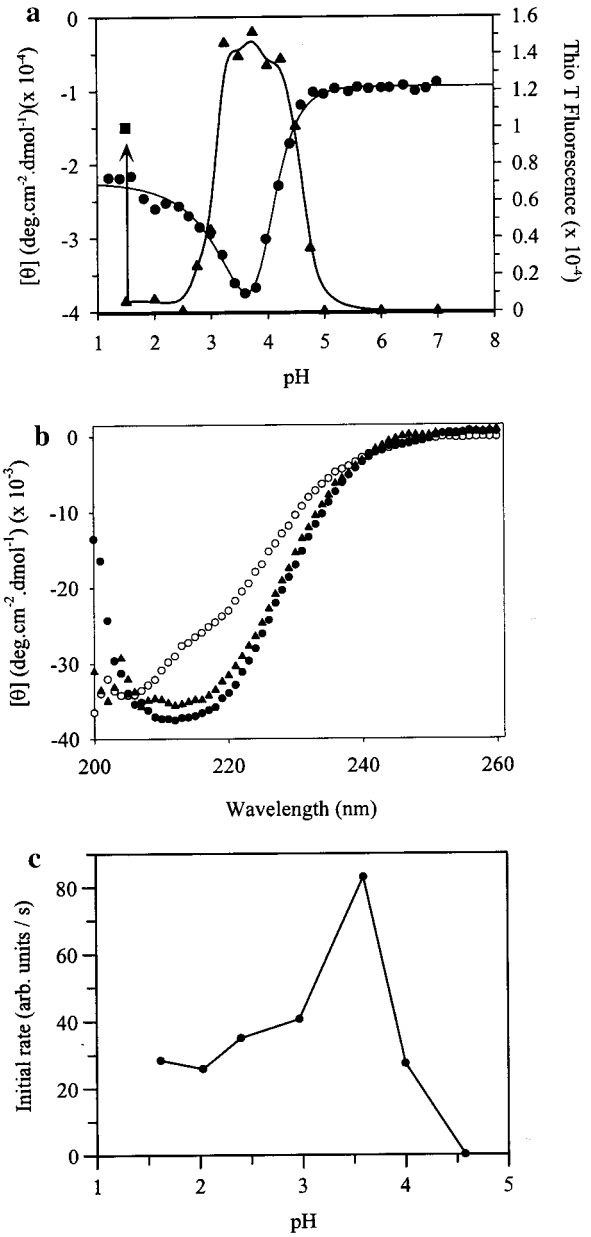

FIGURE 9: Acid denaturation of β_2m and the rate of fibrillogenesis. (a) Acid denaturation of β_2m at 25 °C, monitored after acidification by far-UV CD at 220 nm (closed circle). The CD data are fitted to eq 1 (see Materials and Methods). Thio-T binding was determined (see Materials and Methods) after incubation for 72 h (closed triangles). For one sample at pH 1.2, 0.4 M NaCl was added, and thio-T binding again was measured (filled square). (b) Comparison of the far-UV CD spectra of β_2m at 25 °C at pH 4.0 (filled circle), pH 1.2 (open circle), and pH 1.2 in the presence of 0.4 M NaCl (filled triangle). (c) Effect of pH on the initial rate of fibrillogenesis. β_2m was incubated at different pH values at 25 °C at a constant ionic strength of 400 mM, and the initial rate of fibril formation was estimated from the change in thio-T fluorescence measured in a continuous assay (see Materials and Methods).

vesicles of mesenchymal cells and macrophages (*58*), wherein they also retain the curvilinear appearance of their counterparts formed in vitro. β_2m fibrils thus have a typical morphology that allows them to be easily distinguished from fibrils formed from other proteins (*50, 59*). Fibrils of β_2m have also been formed in vitro, using monomeric protein, by the extension of amyloid fibrils extracted from patients with DRA (*38*). In this case, the fibrils formed were also 6−10 nm wide but are longer and straighter than those

prepared in the present work and described above. This raises the possibility that the assembled material formed here in vitro may represent protofilaments, rather than fully assembled fibrils. In agreement with this view, the β_2m assemblies formed in these studies from recombinant protein are shorter than extended fibrils, soluble (forming gels rather than precipitates), and curvilinear, like the protofilaments found for other proteins and peptides (*17, 18, 60*). Despite exploring a wide range of conditions, however, further assembly of the β_2m to higher order structures or fibrils of straighter morphology has not been observed, even after incubation times of up to 6 months. Further analysis, for example, by cross-sectional analysis (*52*) or atomic force microscopy (*20*), will be needed to dissect the ultrastructure of the β_2m fibrils generated here at acidic pH in vitro.

The data presented here suggest that partially unfolded β_2m is a key intermediate in fibrillogenesis. In support of this conclusion, the initial rate of fibrillogenesis is maximal around pH 3.6, where the population of partially unfolded β_2m is greatest. Below this pH, further unfolding decreases the population of the amyloid precursor and the initial rate of amyloidogenesis is decreased. In addition, acid-unfolded β_2m at pH 1.5 becomes fibrillogenic only upon its refolding induced by the addition of salt. This further supports a crucial role of partially unfolded β_2m in amyloid formation. Partially unfolded β_2m possesses features of a 'molten globule' state (*61*). It thus (i) binds ANS; (ii) is weakly protected from hydrogen exchange; (iii) has significant levels of secondary structure; and (iv) has residual non-native, fixed tertiary interactions. This species is in equilibrium with the native protein and more highly unfolded forms. Conditions which favor the population of the partially unfolded species will thus favor fibrillogenesis, in agreement with the data presented above. Whether fibrils are formed from a specific intermediate or from a number of intermediates displaying an active polymerization face in the ensemble of partially folded states cannot be determined from our measurements. However, it is unlikely that a single, well-defined species, or a single residue, will be responsible for amyloidosis of β_2m or other proteins in isolation. Our data suggest, however, that titration of one or more groups with an average pK_a of 4.7 destabilizes the native protein relative to alternative partially folded conformers. Likely candidates are one or more of the 8 glutamic acid or 7 aspartic acid residues found in β_2m, although other residues with unusually low pK_a values cannot be ruled out. His84 is one such possibility. This residue is buried in the core of the native protein (Figure 1a) and, accordingly, would be expected to have a low pK_a. Indeed, electrostatic calculations suggest this is the case (S. E. Radford, D. Westhead, and J. Nielsen, unpublished results). Asp59 and Glu74 are also possibilities. These residues lie in loops and form salt bridges with residues toward the termini of the protein (Arg3 and Arg97, respectively) (Figure 1a). Interestingly, residues located in a conserved salt bridge in an immunoglobulin light chain have also been shown to be important in amyloidosis, although individual mutations of the residues involved have a variable effect on the mode of aggregation (*28, 29*). Conditions or mutations that destabilize the native protein but maintain population of partially unfolded states have been invoked in the amyloidogenicity of several other proteins, including TTR (*26, 62*), immunoglobulin light chains (*28*−*30*), lysozyme (*25*), acylphosphatase (*35*), and SH3 domains (*34*). Together with the data presented here on β_2m, it appears that both native-state stability and the population of a partially unfolded state(s) are key features in the formation of amyloid from all of these proteins.

Disulfide bonds stabilize the native folds of many extracellular proteins, including the amyloidogenic proteins, immunoglobulin light chains, lysozyme, prions, insulin, and β_2m. In immunoglobulin light chains, reduction of their single disulfide bond leads to facile formation of amyloid fibrils in vitro, consistent with the decrease in stability of the reduced native protein (*63*) and with the general observation that native-state stability and amyloidogenicity are highly correlated phenomena (*25*−*27, 30*). A role for disulfide bond reduction in amyloidosis in vivo, however, has not been shown. Indeed, native, monomeric protein has been recovered from amyloid deposits of human lysozyme (*25*) and β_2m (*2, 3*), suggesting, for these proteins at least, that a significant proportion of the protein in amyloid deposits is in the oxidized form. Moreover, the observation that amyloid can be formed from lysozyme (*25*), immunoglobulin light chains (*64*), insulin (*65*), and β_2m [(*3, 11, 37, 38*) and this work] in their oxidized forms suggests that reduction of these proteins is not a prerequisite for amyloidosis.

We have presented here a case for the population of a partially unfolded intermediate of β_2m as a key precursor in amyloidosis. One question that remains is how might such an intermediate be formed in vivo? During renal failure, β_2m concentrations in serum increase markedly. Because the β_2m shows an affinity for collagen (*66*), the protein accumulates within joints, resulting in the crowding of macrophages into these areas (*5, 67*). Subsequent uptake into lysosomes would expose the protein to a reduced pH environement, favoring the partial unfolding of β_2m. Within the lysosomes, competition between the formation of fibrils and β_2m degradation would then occur. Fibrils that are formed would presumably be secreted and reassociate with collagen within joints, initiating the pathology of DRA. In agreement with this model, β_2m has been shown to dissociate from MHC class I molecules in the acidic environment of early endosomes (*68*), and β_2m fibrils have been observed in lysosomes (*58*). Interestingly, β_2m is also known to stimulate collagenases from osteoblasts (*69*), resulting in joint degradation and eliciting the symptoms of DRA. β_2m fibrils may also form in vivo at neutral pH, in agreement with the observation that fibrils can be formed in vitro at close to neutral pH by dialysis procedures (*3, 11, 37*). Under these conditions, partially unfolded molecules would be rarely, and transiently, populated by dynamic excursions from the native state. As a consequence, the probability of intermolecular interactions would be dramatically reduced and the rate of amyloidosis substantially decreased, in agreement with the data presented above. Much remains to be learned about the development of the β_2m amyloid in vivo, but it is clear that insights into the conformational dynamics of the β_2m at the molecular level, such as those described above, may pave the way for future intervention in the progression of this and other amyloid diseases.

ACKNOWLEDGMENT

We thank Paul Varley for providing material and help at the outset of this project, Nigel Woods and Keith Ainley

for help with microbiological growths and protein preparations, Alison Ashcroft for mass spectrometry experiments, and Andrew Sharff for assistance with X-ray data collection. We thank John Bell and Vittorio Bellotti for providing the plasmid pNH1+. We also thank Geoff Howlett, Colin Rieger, and Andy Baron for analytical ultracentrifugation experiments; Les Child for photography; David Smith for help with Figure 1; Paul McPhie for EM advice; and Steve Homans and the S.E.R. group for helpful discussions.

REFERENCES

1. Sipe, J. D. (1992) *Annu. Rev. Biochem. 61*, 947−975.
2. Bellotti, V., Stoppini, M., Mangione, P., Sunde, M., Robinson, C., Asti, L., Brancaccio, D., and Ferri, G. (1998) *Eur. J. Biochem. 258*, 61−67.
3. Campistol, J. M., Bernard, D., Papastoitsis, G., Sole, M., Cohen, A. S., and Skinner, M. (1994) *Kidney Int. 46*, 577.
4. Gejyo, F., Yamada, T., Odani, S., Nakagawa, Y., Arakawa, M., Kunitomo, T., Kataoka, H., Suzuki, M., Hirasawa, Y., Shirahama, T., Cohen, A. S., and Schmid, K. (1985) *Biochem. Biophys. Res. Commun. 129*, 701−706.
5. Ayers, D. C., Athanasou, N. A., Woods, C. G., and Duthie, R. B. (1993) *Clin. Orthop. Relat. Res. 290*, 216−224.
6. Van Ypersele, C., and Drucke, T. B. (1996) in *Dialysis Amyloid*, pp 34−68, Oxford University Press, New York.
7. Bjorkman, P. J., Saper, M. A., Samaoui, B., Bennett, W. S., Strominger, J. L., and Wiley, D. C. (1987) *Nature 329*, 506−512.
8. Gejyo, F., Homma, N., Suzuki, Y., and Arakawa, M. (1986) *N. Engl. J. Med. 314*, 585−586.
9. Tan, S. Y., and Pepys, M. B. (1994) *Histopathology 25*, 403−414.
10. Linke, R. P., Kerling, A., and Rail, A. (1993) *Kidney Int. 43*, S100−S105.
11. Ono, K., and Uchino, F. (1994) *Nephron 66*, 404−407.
12. Yamada, T., Kakihara, T., Gejyo, F., and Okada, M. (1994) *Ann. Clin. Lab. Sci. 24*, 243−249.
13. Argiles, A. (1996) *Nephrology 2*, 373−386.
14. Miyata, T. (1993) *J. Clin. Inv. 92*, 1243−1252.
15. Davison, A. M. (1995) *Contrib. Nephrol. 113*, 92−100.
16. Sunde, M., Serpell, L. C., Bartlam, M., Fraser, P. E., Pepys, M. B., and Blake, C. C. F. (1997) *J. Mol. Biol. 273*, 729−739.
17. Harper, J. D., Lieber, C. M., and Lansbury, P. T. (1997) *Chem. Biol. 4*, 951−959.
18. Harper, J. D., Wong, S. S., Lieber, C. M., and Lansbury, P. T. (1997) *Chem. Biol. 4*, 119−125.
19. Walsh, D. M., Lomakin, A., Benedek, G. B., Condron, M. M., and Teplow, D. B. (1997) *J. Biol. Chem. 272*, 22364−22372.
20. Ionescu-Zanetti, C., Khurana, R., Gillespie, J. R., Petrick, J. S., Trabachino, L. C., Minert, L. J., Carter, S. A., and Fink, A. L. (1999) *Proc. Natl. Acad. Sci. U.S.A. 96*, 13175−13179.
21. Klunk, W. E., Jacob, R. F., and Mason, R. P. (1999) *Methods Enzymol. 309*, 285−305.
22. Puchtler, H., Sweat, F., and Levine, M. (1962) *J. Histochem. Cytochem. 10*, 355−364.
23. Levine, H. (1995) *Amyloid 2*, 1−6.
24. Naiki, H., Higuchi, K., Hosokawa, M., and Takeda, T. (1989) *Anal. Biochem. 177*, 244−249.
25. Booth, D. R., Sunde, M., Bellotti, V., Robinson, C. V., Hutchinson, W. L., Fraser, P. E., Hawkins, P. N., Dobson, C. M., Radford, S. E., Blake, C. C. F., and Pepys, M. B. (1997) *Nature 385*, 787−793.
26. Lai, Z. H., Colon, W., and Kelly, J. W. (1996) *Biochemistry 35*, 6470−6482.
27. McCutchen, S. L., Lai, Z. H., Miroy, G. J., Kelly, J. W., and Colon, W. (1995) *Biochemistry 34*, 13527−13536.
28. Hurle, M. R., Helms, L. R., Li, L., Chan, W. N., and Wetzel, R. (1994) *Proc. Natl. Acad. Sci. U.S.A. 91*, 5446−5450.
29. Helms, L. R., and Wetzel, R. (1996) *J. Mol. Biol. 257*, 77−86.
30. Raffen, R., Dieckman, L. J., Szpunar, M., Wunschl, C., Pokkuluri, P. R., Dave, P., Stevens, P. W., Cai, X. Y., Schiffer, M., and Stevens, F. J. (1999) *Protein Sci. 8*, 509−517.
31. Hosszu, L. L. P., Baxter, N. J., Jackson, G. S., Power, A., Clarke, A. R., Waltho, J. P., Craven, C. J., and Collinge, J. (1999) *Nat. Struct. Biol. 6*, 740−743.
32. Jackson, G. S., Hosszu, L. L. P., Power, A., Hill, A. F., Kenney, J., Saibil, H., Craven, C. J., Waltho, J. P., Clarke, A. R., and Collinge, J. (1999) *Science 283*, 1935−1937.
33. Hornemann, S., Korth, C., Oesch, B., Riek, R., Wider, G., Wuthrich, K., and Glockshuber, R. (1997) *FEBS Lett. 413*, 277−281.
34. Guijarro, J. I., Sunde, M., Jones, J. A., Campbell, I. D., and Dobson, C. M. (1998) *Proc. Natl. Acad. Sci. U.S.A. 95*, 4224−4228.
35. Chiti, F., Webster, P., Taddei, N., Clark, A., Stefani, M., Ramponi, G., and Dobson, C. M. (1999) *Proc. Natl. Acad. Sci. U.S.A. 96*, 3590−3594.
36. Ratnaswamy, G., Koepf, E., Bekele, H., Yin, H., and Kelly, J. (1999) *Chem. Biol. 6*, 293−304.
37. Connors, L. H., Shirahama, T., Skinner, M., Fenves, A., and Cohen, A. S. (1985) *Biochem. Biophys. Res. Commun. 131*, 1063−1068.
38. Naiki, H., Hashimoto, N., Suzuki, S., Kimura, H., Nakakuki, K., and Gejyo, F. (1997) *Amyloid 4*, 223−232.
39. Reid, S. W., Smith, K. J., Jakobsen, B. K., O'Callaghan, C. A., Reyburn, H., Harlos, K., Stuart, D. I., McMicheal, A. J., Bell, J. I., and Jones, E. Y. (1996) *FEBS Lett. 383*, 119−123.
40. Ezaz-Nikpay, K., Uchino, K., Lerner, R. E., and Verdine, G. L. (1994) *Protein Sci. 3*, 132−138.
41. Burgess, R. R. (1996) *Methods Enzymol. 273*, 245−249.
42. Garboczi, D. C., Wiley, D. C., and Hung, D. T. (1992) *Proc. Natl. Acad. Sci. U.S.A. 89*, 3429−3433.
43. Sunde, M., and Blake, C. (1997) *Adv. Protein Chem. 50*, 123−159.
44. Fink, A. L., Calciano, L. J., Goto, Y., Kurotsu, T., and Palleros, D. R. (1994) *Biochemistry 33*, 12504−12511.
45. Okon, M., Bray, P., and Vucelic, D. (1992) *Biochemistry 31*, 8906−8915.
46. Bai, Y., Milne, J. S., Mayne, L., and Englander, S. W. (1993) *Proteins: Struct., Funct., Genet. 17*, 75−86.
47. Aggeli, A., Bell, M., Boden, N., Keen, J. N., Knowles, P. F., McLeish, T. C. B., Pitkeathly, M., and Radford, S. E. (1997) *Nature 386*, 259−262.
48. Stine, W. B., Snyder, S. W., Ladror, U. S., Wade, W. S., Miller, M. F., Perun, T. J., Holzman, T. F., and Krafft, G. A. (1996) *J. Protein Chem. 15*, 193−203.
49. Shirahama, T., and Cohen, A. S. (1965) *Nature 206*, 737−738.
50. Nishi, S., Ogino, S., Maruyama, Y., Honma, N., Gejyo, F., Morita, T., and Arakawa, M. (1990) *Nephron 56*, 357−363.
51. Blake, C., and Serpell, L. (1996) *Structure 4*, 989−998.
52. Serpell, L. C., Sunde, M., Fraser, P. E., Luther, P. K., Morris, E. P., Sangren, O., Lundgren, E., and Blake, C. C. F. (1995) *J. Mol. Biol. 254*, 113−118.
53. Woody, R. W. (1995) *Methods Enzymol. 246*, 34−71.
54. Semisotnov, G. V., Rodionova, N. A., Razgulyaev, O. I., Uversky, V. N., Gripas, A. F., and Gilmanshin, R. I. (1991) *Biopolymers 31*, 119−128.
55. Harper, J. D., Wong, S. S., Lieber, C. M., and Lansbury, P. T. (1999) *Biochemistry 38*, 8972−8980.
56. Wood, S. J., Maleeff, B., Hart, T., and Wetzel, R. (1996) *J. Mol. Biol. 256*, 870−877.
57. Lashuel, H. A., Wurth, C., Woo, L., and Kelly, J. W. (1999) *Biochemistry 38*, 13560−13573.
58. GarciaGarcia, M., Argiles, A., GouinCharnet, A., Durfort, M., GarciaValero, J., and Mourad, G. (1999) *Kidney Int. 55*, 899−906.
59. Inoue, S., Kuroiwa, M., Ohashi, K., Hara, M., and Kisilevsky, R. (1997) *Kidney Int. 52*, 1543−1549.
60. Goldsbury, C. S., Cooper, G. J. S., Goldie, K. N., Muller, S. A., Saafi, E. L., Gruijters, W. T. M., and Misur, M. P. (1997) *J. Struct. Biol. 119*, 17−27.
61. Ptitsyn, O. B. (1995) *Curr. Opin. Struct. Biol. 5*, 74−78.

62. Colon, W., and Kelly, J. W. (1992) *Biochemistry 31*, 8654−8660.
63. Frisch, C., Kolmar, H., and Fritz, H. J. (1994) *Biol. Chem. Hoppe−Seyler 375*, 353−356.
64. Stevens, P. W., Raffen, R., Hanson, D. K., Deng, Y. L., Berrioshammond, M., Westholm, F. A., Murphy, C., Eulitz, M., Wetzel, R., Solomon, A., Schiffer, M., and Stevens, F. J. (1995) *Protein Sci. 4*, 421−432.
65. Burke, M. J., and Rougvie, M. A. (1972) *Biochemistry 11*, 2435−2439.
66. Homma, N., Gejyo, F., Isemura, M., and Arakawa, M. (1989) *Nephron 53*, 37−40.
67. Ohashi, K., Hara, M., Kawai, R., Ogura, Y., Honda, K., Nihei, H., and Mimura, N. (1992) *Kidney Int. 41*, 1646−1652.
68. Hochman, J. H., Jiang, H., Matyus, L., Edidin, M., and Pernis, B. (1991) *J. Immun. 146*, 1862−1867.
69. Brinckerhoff, C. E., Mitchell, T. I., Karmilowicz, M. J., Kluvebeckerman, B., and Benson, M. D. (1989) *Science 243*, 655−657.

BI000276J